ORIGINAL PAPER

Conductance hysteresis in the voltage-dependent anion channel

Shay M. Rappaport[1] · Oscar Teijido[1] · David P. Hoogerheide[1,2] ·
Tatiana K. Rostovtseva[1] · Alexander M. Berezhkovskii[1,3] · Sergey M. Bezrukov[1]

Abstract Hysteresis in the conductance of voltage-sensitive ion channels is observed when the transmembrane voltage is periodically varied with time. Although this phenomenon has been used in studies of gating of the voltage-dependent anion channel, VDAC, from the outer mitochondrial membrane for nearly four decades, full hysteresis curves have never been reported, because the focus was solely on the channel opening branches of the hysteresis loops. We studied the hysteretic response of a multichannel VDAC system to a triangular voltage ramp the frequency of which was varied over three orders of magnitude, from 0.5 mHz to 0.2 Hz. We found that in this wide frequency range the area encircled by the hysteresis curves changes by less than a factor of three, suggesting broad distribution of the characteristic times and strongly non-equilibrium behavior. At the same time, quasi-equilibrium two-state behavior is observed for hysteresis branches corresponding to VDAC opening. This enables calculation of the usual equilibrium gating parameters, gating charge and voltage of equipartitioning, which were found to be almost insensitive to the ramp frequency. To rationalize this peculiarity, we hypothesize that during voltage-induced closure and opening the system explores different regions of the complex free energy landscape, and, in the opening branch, follows quasi-equilibrium paths.

Introduction

The voltage-dependent anion channel, VDAC, the major protein of the mitochondrial outer membrane, is known to be responsible for most of the metabolite exchange across the membrane. When reconstituted in lipid bilayers, this 32-kDa membrane protein forms a monomeric beta-barrel channel of 4 ± 0.1 nS conductance in 1 M KCl. The characteristic and conserved property of the channel is voltage gating. Under applied voltages of $|V| > 30$ mV the channel undergoes transitions between a high-conducting open state and the so-called "closed" states characterized by a variety of less-conducting conformations (Colombini 1989, 2012; Schein et al. 1976). Although voltage gating of beta-barrel channels, for example bacterial porins and several toxins (Arbing et al. 2001; Bainbridge et al. 1998b; Bowen et al. 1985; Bredin et al. 2002; Brunen and Engelhardt 1993; Delcour et al. 1989; Nestorovich et al. 2003; Schindler and Rosenbusch 1978; VanGelder et al. 1997), has long been recognized as a common intrinsic property (Bainbridge et al. 1998a; Robertson and Tieleman 2002; Zachariae et al. 2012), the underlying molecular mechanisms of this intriguing phenomenon are still debated. Moreover, it is not even clear how much they have in common.

S. M. Rappaport and O. Teijido contributed equally to the study.

✉ Sergey M. Bezrukov
  bezrukos@mail.nih.gov

1 Program in Physical Biology, Eunice Kennedy Shriver National Institute of Child Health and Human Development, National Institutes of Health, Bethesda, MD 20892, USA

2 Center for Neutron Research, National Institute of Standards and Technology, Gaithersburg, MD 20899, USA

3 Mathematical and Statistical Computing Laboratory, Division for Computational Bioscience, Center for Information Technology, National Institutes of Health, Bethesda, MD 20892, USA

Due to the special role of VDAC in mitochondrial homeostasis, its gating is among the most studied. Diverse current ideas on the mechanism of beta-barrel channel gating include motion of the external loops that connect the beta-strands of the barrels (Arbing et al. 2001; Brunen and Engelhardt 1993; Soares et al. 1995; Watanabe et al. 1997), some kind of crucial perturbation of the electrostatic field distribution inside the channel lumen (Bainbridge et al. 1998a; Robertson and Tieleman 2002), and large voltage-induced conformational changes of protein structure (Colombini 1989; Zachariae et al. 2012). In what concerns VDAC, the most developed model of gating (Colombini 2012; Peng et al. 1992; Song et al. 1998; Thomas et al. 1993) proposes voltage-induced large structural rearrangements of the channel. This model is supported by the high sensitivity of the channel to osmotic stress (Zimmerberg and Parsegian 1986).

The functional role of gating is backed by the finding that ATP translocates through a VDAC's open state but not through its closed states (Rostovtseva and Colombini 1996, 1997). Therefore, by gating, VDAC is able to increase or reduce both ATP delivery to the cytosol and ADP access to the electron transport chain complexes in the mitochondrial inner membrane, thus directly affecting mitochondrial energy conversion. According to this model, VDAC closure limits mitochondrial oxidative phosphorylation whereas VDAC opening favors it. Any restriction of metabolite exchange through VDAC could lead to disturbance of mitochondrial energetic function and cell metabolism (Lemasters and Holmuhamedov 2006; Lemasters et al. 2012). The high abundance of VDAC in the mitochondrial outer membrane is believed to cause significant dissipation of the transmembrane potential, thus inciting long-standing debates about the physiological relevance of voltage-induced gating (Colombini 2004, 2012; Rostovtseva and Bezrukov 2012). However, the Donnan potential that arises because of the high concentration of charged macromolecules (e.g., cytochrome c with +9 charges), to which VDAC is not permeable, in the mitochondrial intermembrane space at the outer membrane surface could be a source of potentials estimated to be between 10 and 20 mV (Lemeshko 2006) or even as high as 46 mV (Porcelli et al. 2005). One new model even suggests generation of trans-outer-membrane potentials as high as 50 mV by VDAC complexes with hexokinase (Lemeshko 2014a, b). Moreover, VDAC gating in vivo could be significantly facilitated by substantial osmotic effects arising from the crowded environment of the cell (Zimmerberg and Parsegian 1986).

VDAC gating is remarkably complex (Colombini 2012). Nevertheless, reproducible dependence of the gating on such environmental conditions as pH (Bowen et al. 1985; Ermishkin and Mirzabekov 1990; Teijido et al. 2014), osmotic pressure (Zimmerberg and Parsegian 1986), presence of poly-anions (Colombini 1989; Mangan and

Colombini 1987), and membrane lipid content (Rostovtseva et al. 2006), among others, has been reported, which necessitates some means of their empirical quantitative characterization.

Assuming that the channel is a two-state equilibrium system, gating is usually characterized by two parameters: gating charge and the characteristic voltage of equipartitioning (half-effect) between the open and closed states (Ehrenstein et al. 1970; Hille 2001). When voltage changes with time, such a description is still applicable if the rate of voltage variation is low enough to ensure "instantaneous" equilibration of the channel. Colombini and coworkers applied this simple description to VDAC gating on the basis of the observation that, at the decreasing voltages corresponding to channel opening, equilibrium-like behavior of the channels was observed (Schein et al. 1976; Zizi et al. 1995, 1998). In particular, they demonstrated that changing the frequency of the periodic triangular wave of the voltage from 0.5 to 5 mHz did not change the "opening" branches of the properly normalized multichannel current–voltage dependences, which were satisfactorily described by a two-state model of channel voltage gating. Although this analysis has been systematically used to study VDAC gating for the last four decades (see, e.g., a recent review article by Colombini (2012) and references therein), to our knowledge full hysteresis curves have never been reported in the literature.

The objective of this study was to examine VDAC conductance hysteresis in a wide frequency range in an attempt to reconcile the recognized complexity of VDAC gating with the simplicity of its well-accepted characterization in terms of a two-state equilibrium model for the opening branches of the hysteresis curves. In our analysis we used a comparison with a two-state Markov model, not only because of this quasi-equilibrium behavior, but also because analytical results for the hysteresis area are available for this model only (Pustovoit et al. 2006). We found that the hysteresis curves were characterized by a complex shape that could be interpreted as the result of very fast channel opening and very slow closure, with a characteristic time that exceeded the longest period of the applied voltage ramp (2000 s) used in our experiments. This is in agreement with previous findings by Schein et al. (1976), who mentioned the complexity of VDAC response to voltage and, in particular, showed that relaxation toward voltage-induced VDAC closure is much slower than relaxation toward its opening on return to virtual zero voltage. However, we point out that such behavior can be expected, even for the simplest possible case of a two-state Markov model, if the rate constants are functions of the voltage. We performed a crucial experiment on relaxation to the *same* voltage from two different initial voltages. For a two-state Markov model, this relaxation is expected to be

characterized by a single exponent with a relaxation time independent of the initial conditions. The results of our experiment showed that the relaxation times can be different by orders of magnitude, which clearly demonstrates the failure of the two-state model to grasp the remarkable complexity of VDAC gating. To rationalize the complex gating behavior of VDAC, we speculate that the channels explore distinctly different regions of their free energy landscape, one on the way to the voltage-induced closure and the other on the way to opening, when the channels are close to equilibrium.

Materials and methods

Planar lipid membranes were formed on orifices of 70–90 μm in diameter in a 15 μm thick Teflon partition that separated two compartments (Rostovtseva et al. 2006). Briefly, the cis and trans compartments were filled with 1.2 mL aqueous 1 M KCl (M = mol/l) buffered with 5 mM HEPES at pH 7.4. Lipid monolayers used for membrane formation were prepared from a 5-mg/ml solution of 95 % asolectin and 5 % cholesterol in pentane (Avanti Polar Lipids, Albaster, AL, USA). Teflon orifices were pretreated with petroleum jelly. Channel insertion was achieved by adding 0.1–0.3 μl of ~0.1 μg/μl VDAC solution in 2.5 % Triton X-100 to the cis compartment while stirring. VDAC was isolated from rat liver mitochondria. Potential was defined as positive when it was greater at the cis side. Channel incorporation into the membrane usually took 20–30 min, after which conductance reached an acceptable steady-state. Current recordings were performed, as described elsewhere (Rostovtseva et al. 2006), by use of an Axopatch 200B amplifier (Axon Instruments, Foster City, CA, USA) in the voltage-clamp mode.

Hysteresis experiments were performed by use of periodic triangular waves from a Function Waveform Generator 33120A (Hewlett Packard) with voltage changing from 0 to −60 mV and back in the frequency range 0.5 mHz–0.2 Hz. Data were acquired with a Digidata 1322A board (Axon Instruments) at sampling frequencies ranging from 1 Hz to 5.0 kHz, with a low-pass Bessel filter set to 1.0 kHz, and analyzed by use of pClamp 10.2 software (Axon Instruments). Relaxation experiments used voltage protocols described in the figure captions.

Results and discussion

Although the response of multichannel VDAC conductance to decreasing voltage (channel opening) has been extensively studied (Colombini 1989; Mangan and Colombini 1987; Rostovtseva et al. 2006; Schein et al. 1976; Teijido et al. 2014; Zizi et al. 1995, 1998), as far as we are aware

full hysteresis curves have never been published. We therefore studied the conductance of multichannel membranes in response to a voltage ramp (piecewise linear voltage vs. time). An example of the 20 mHz ramp with voltage changing between 0 and −60 mV is given in the bottom panel of Fig. 1a. The current response of a membrane containing ~70 VDAC channels is shown in the upper panel. The response is sub-linear, as is apparent from reproducible deviations of the current from the initial straight lines at small voltages.

Figure 1b shows the relative conductance of a membrane with approximately one hundred VDAC channels as a function of the instantaneous voltage of piecewise linear ramps at 5 different ramp frequencies ranging from 0.5 mHz to 0.2 Hz. Each hysteresis loop is an average over several voltage cycles. The relative conductance is defined as the ratio $G(V)/G(0)$, where $G(V)$ is the instantaneous multichannel membrane conductance at a given voltage, $G(V) = I(V)/V$, and $G(0)$ is the conductance at zero applied voltage corresponding to the beginning of each cycle. It is important to note here that the experiment shows that the value of $G(0)$ is independent of ramp frequency. The only purpose of such normalization is to facilitate comparison of the data obtained in different experiments and in the course of long experiments with several repeated ramp applications by eliminating long-term variations because of the gradual change in the number of VDAC channels in the bilayer. It is apparent that the conductance response to a particular instantaneous voltage is frequency-dependent, specifically, the slower the voltage change, the stronger the response. For example, the 0.2 Hz ramp leads to only approximately 10 % reduction of the conductance from its value measured at zero voltage whereas the 0.5 mHz ramp induces a reduction of conductance of approximately 40 %. Thus, at voltages in the range of −60 to −50 mV, the slowest ramp used in our experiment has an effect on channel conductance approximately fourfold larger than the fastest ramp. Interestingly, one of the features of VDAC channel response to the periodically varying piecewise linear voltage is that the system returns to the same initial "conductance of zero applied voltage" after each cycle for the entire frequency range, from 0.5 mHz to 0.2 Hz, so that $G(0)$ is independent of ramp frequency (data not shown).

Analysis of hysteretic behavior has proved to be a useful tool in studies of ion channels (Andersson 2010; Banerjee 2015; Das et al. 2012; Flyvbjerg et al. 2012; Fologea et al. 2011; Juraszek et al. 2005; Kaestner et al. 2000; Mannikko et al. 2005; Mathes and Engelhardt 1998; Pustovoit et al. 2006; Zhou et al. 1998). One way used to characterize hysteresis is to examine the area encircled by the curves as a function of the ramp frequency. The symbols in Fig. 1c are the loop areas calculated from the data in Fig. 1b (circles) and similar measurements performed on multichannel

Fig. 1 Conductance of a multichannel membrane with a voltage ▶ ramp frequency ranging from 0.5 mHz to 0.2 Hz shows sensitivity of the hysteresis curves to the ramp frequency. **a** Raw data for ion current through a multichannel system of approximately 70 VDAC channels (*upper panel*) in response to a 0 to −60 mV voltage ramp of 20 mHz frequency (*lower panel*). **b** Conductance hysteresis curves for different frequencies of the ramp. The *arrows* on the 0.2 Hz trace show the direction of the voltage change in the parts of the hysteresis loop corresponding to channel closing and opening. The data were averaged over several ramp periods. **c** The areas *encircled* by the hysteresis *curves* as a function of the ramp frequency. The areas calculated from three independent experiments on multi-channel membranes containing 70–180 channels are shown by use of *different symbols*. The area does not tend to decrease at low frequencies, suggesting large deviations from equilibrium and the existence of a broad range of relaxation times, including times exceeding $1/(0.5\ \text{mHz}) = 2000$ s. The *solid line* through the data is the best fit to the equation $A(f) = A_0/(f/f_0 + f_0/f)$, with A_0 and f_0 used as adjustable parameters

membranes (squares and triangles). It is apparent that the change in the loop area does not exceed a factor of three throughout the range of ramp frequencies.

Figure 2a shows the hysteresis curves of Fig. 1b after the following transformation, traditionally used in VDAC gating analysis (Zizi et al. 1998):

$$G_{\text{norm}}(V) = [G(V) - G_{\text{min}}]/[G(0) - G_{\text{min}}], \quad (1)$$

where G_{min} is the minimum conductance within a particular ramp cycle. Essentially, this transformation excludes the population of the channels which did not have enough time to close, so the $G(V(t)) - G_{\text{min}}$ term mostly accounts for the channels that had "gated" to the closed states. It has an advantage that $G_{\text{norm}}(V)$ enables quantitative description of voltage-induced gating. It is apparent that while the descending, "closing" branches remain distinctly different from each other, depending on the voltage ramp frequency, the ascending, "opening" branches of the VDAC conductance response group together.

Quantitative analysis of equilibrium channel voltage gating is most often carried out within the framework of a two-state model. This model describes the voltage-dependent equilibrium between the two states using two parameters, the effective gating charge n and the voltage of channel equipartitioning between the open and closed conformations, or the "voltage of half-effect" V_0 (Ehrenstein et al. 1970; Hille 2001). It is important that, for VDAC, only the opening branches of the hysteresis curves are used, assuming that $G_{\text{norm}}(V)$ is the equilibrium probability $P_O^{\text{eq}}(V)$ of finding the channel open (Zizi et al. 1998). The latter is given by the Boltzmann distribution:

$$G_{\text{norm}}(V) = P_O^{\text{eq}}(V) = \left\{ 1 + \exp\left[ne(|V| - V_0)/(k_B T) \right] \right\}^{-1}, \quad (2)$$

where e is the elementary charge and k_B and T have their usual meanings of the Boltzmann constant and absolute temperature, respectively. The gating parameters obtained
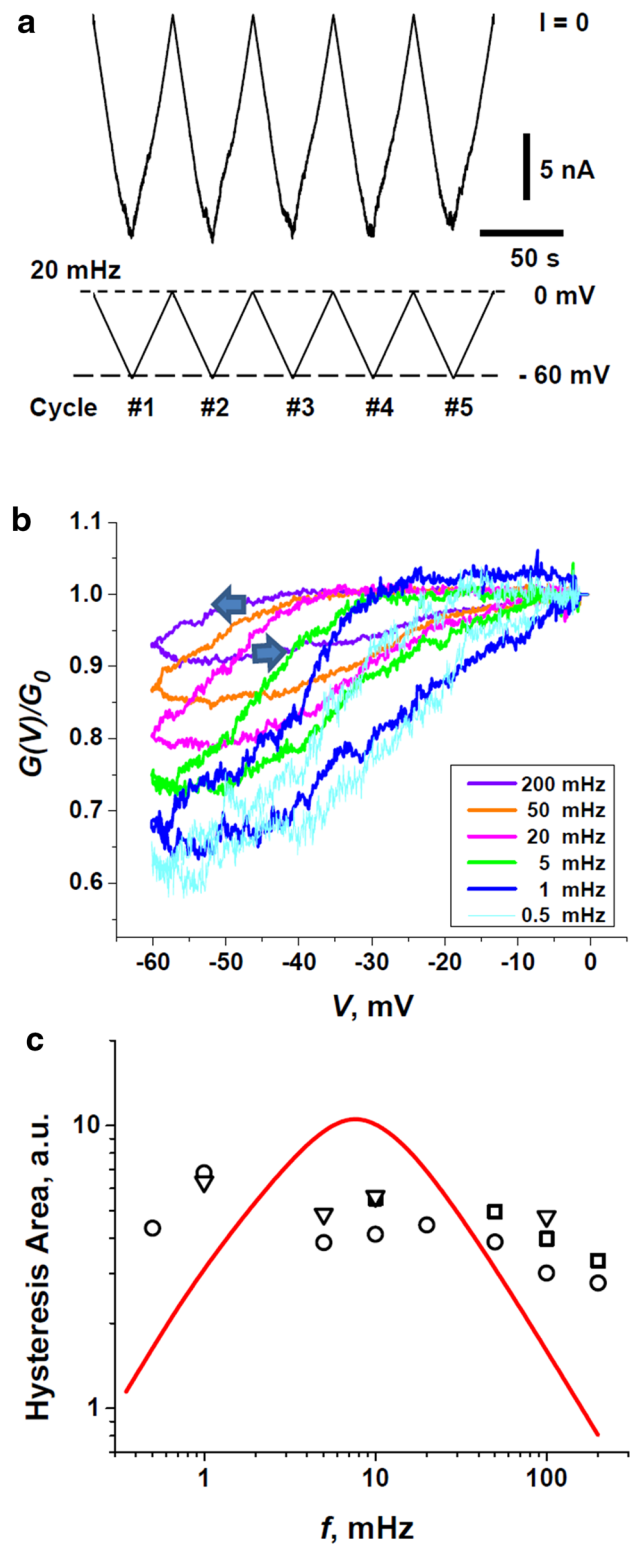
by fitting the experimental data for the ascending branches in Fig. 2a to the voltage dependence in Eq. (2) are shown in Fig. 2b. The values of the gating parameters were almost insensitive to the rate of voltage change. Indeed, both the gating charge, n, and the characteristic potential, V_0, do not deviate by more than 15 % from their average values of
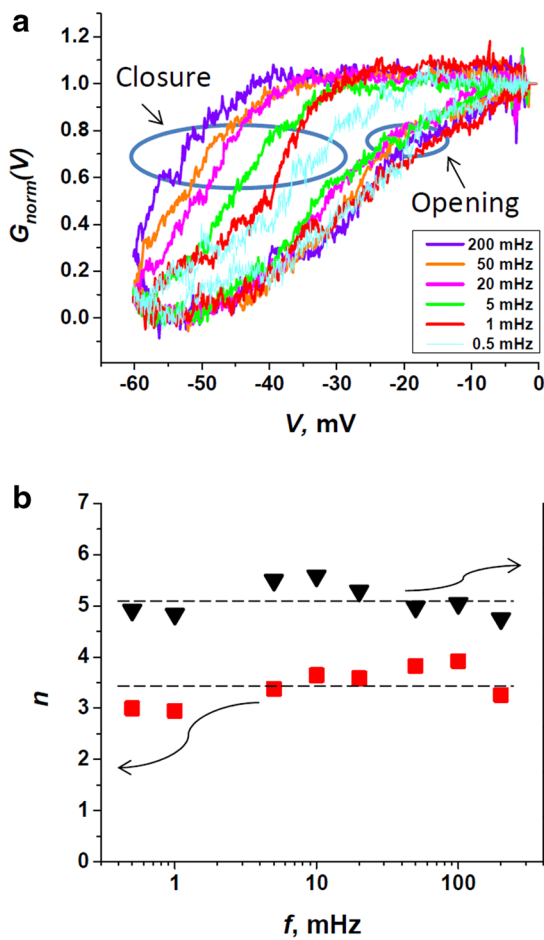
Fig. 2 Normalized hysteresis *curves* show that whereas closure of the channels is highly frequency-dependent, the normalized traces for the opening branches almost overlap. **a** Conductance hysteresis curves of Fig. 1b after transformation by use of Eq. (1). **b** Gating parameters, gating charge n and the voltage of the half-effect V_0 corresponding to $P_O = 0.5$, obtained from fitting the opening branches data to Eq. (2). The *wavy arrows* indicate that the *triangles* and *squares* give the values of V_0 and n, respectively

$n = 3.4 \pm 0.4$ and $V_0 = 29 \pm 3$ mV over the whole range of ramp frequencies, from 0.5 mHz to 0.2 Hz. These values agree with those obtained by Zizi et al. (1998), who analyzed the opening branches at ramp frequencies of 0.5 and 5 mHz under similar conditions.

Universal quasi-equilibrium behavior of the channels on the opening branches of the hysteresis loops suggests "instantaneous" channel equilibration on these branches. Thus the relaxation rates of channel closure and reopening are hugely different, as reported elsewhere (Colombini 2012; Schein et al. 1976). This drastic difference between the two rates is also evident in standard relaxation experiments on the conductance response to abrupt changes in the applied voltage. Figure 3a shows relaxation of multichannel membrane conductance after stepwise application
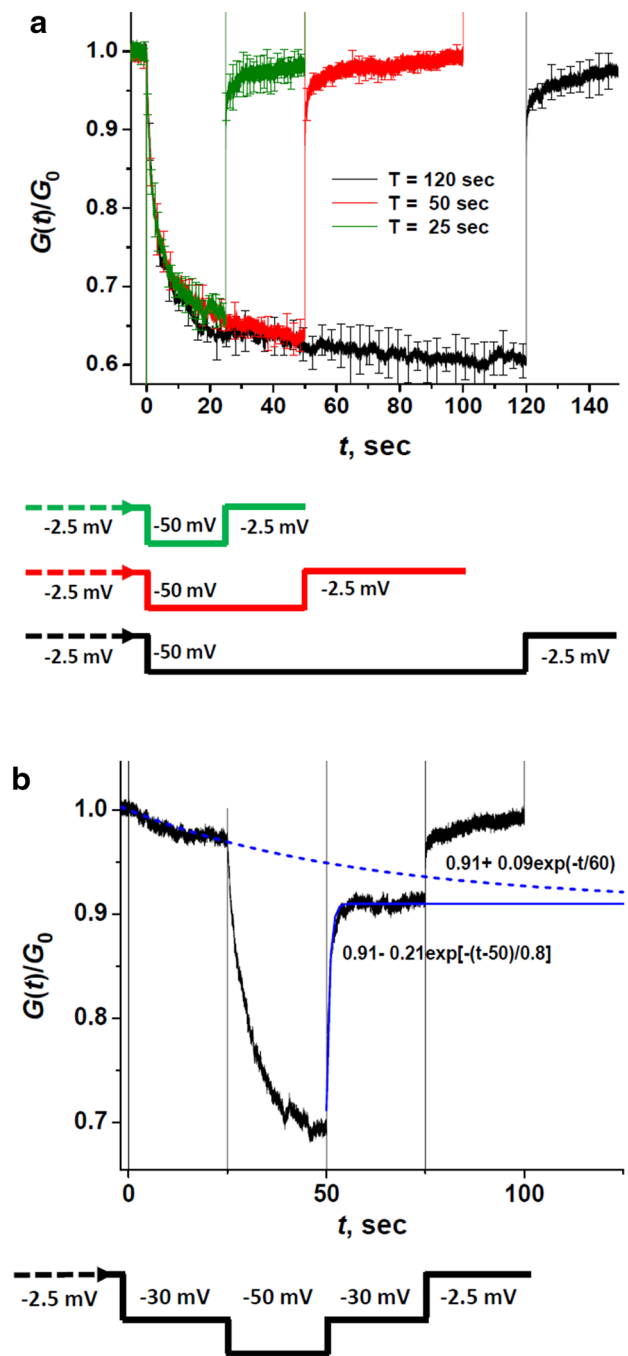

Fig. 3 Two types of relaxation experiment. **a** Conductance relaxation to two different voltages. The voltage protocol, shown at the *bottom*, is to start at −2.5 mV, then apply −50 mV for the three durations shown in the *figure*, and then return to −2.5 mV. Quite different rates of relaxation toward closure and opening are apparent, as might be expected even for a two-state model with voltage-dependent rate constants. **b** Conductance relaxation to the same voltage. Experiments are started at −2.5 mV, then −30 mV is applied, in 25 s the voltage is switched to −50 mV, 25 s later the voltage is returned to −30 mV and then, in 25 s, to −2.5 mV. *Dashed* and *solid lines* are best fits by single exponentials, with the equations displayed in the figure. They show a difference in relaxation times of approximately two orders of magnitude. The data in **a** and **b** are averages from 3 and 4 separate experiments with membranes containing from 80 to 240 channels. The signal was filtered by use of a low-pass Bessel filter at 1.0 kHz and sampled at 5.0 kHz

of −50 mV for different periods of time (25, 50, and 120 s) followed by stepwise return to the near-zero initial voltage of −2.5 mV. (This residual small potential is necessary for reliable monitoring of the membrane "conductance at zero voltage".) In agreement with the findings of Schein et al. (1976), it is clearly seen that the rates of channel closure and opening are quite different. Analysis of the data shows that the characteristic relaxation time, defined as the time necessary to reach $1/e$ level of the difference between the initial conductance and its long-term asymptote is approximately 3 s for closure. For opening, the relaxation time is approximately 7 ms. These values do not depend substantially on system preparation (e.g., on how long it was kept at a particular voltage) but are sensitive to the voltage step amplitude (data not shown).

Although the major part of the relaxation, specifically, about 75 % of the total amplitude, is well approximated by a single exponential function, more thorough analysis of the curves reveals that they have more complex time dependences. For both channel closure and opening there are relaxation tails with additional slow components of at least hundreds of seconds. Considering the long known fact that the "closed" state of VDAC is actually represented by a broad distribution of sub-states with distinctly different conductances and selectivities (Zhang and Colombini 1990), it is natural to expect such multi-exponential behavior. Yet, as follows from Fig. 3a, for voltage jumps to −50 mV and back the relaxation is mainly single-exponential, but occurs on time scales that are different by approximately three orders of magnitude.

It is worth noting that this large difference in relaxation times for channel closing and opening does not, per se, contradict the two-state model of gating. For a population of N identical, uncorrelated two-state channels that switch stochastically between two conductances g_O and g_C of the channel open and closed states, respectively, the time-dependent conductance is a linear function of the probability of finding the channel in the open state at time t, $P_O(t)$, that can be written as (Pustovoit et al. 2006):

$$G(t) = N\left[g_C + (g_O - g_C)P_O(t)\right]. \tag{3}$$

If the channels are Markovian, the probability $P_O(t)$ obeys the rate equation:

$$\frac{dP_O(t)}{dt} = -k_O(t)P_O(t) + k_C(t)[1 - P_O(t)], \tag{4}$$

where $k_O(t)$ and $k_C(t)$ are the time-dependent rate coefficients for transitions between the open and closed states:

$$O \underset{k_C(t)}{\overset{k_O(t)}{\rightleftharpoons}} C. \tag{5}$$

The solution for the time-dependent open state probability is given by (Pustovoit et al. 2006):

$$P_O(t) = P_O(0) \exp\left[-\int_0^t k(t_1)\, dt_1\right]$$
$$+ \int_0^t k_C(t_1) \exp\left[-\int_{t_1}^t k(t_2)\, dt_2\right] dt_1, \tag{6}$$

where:

$$k(t) = k_O(t) + k_C(t). \tag{7}$$

When the time-dependent rate coefficients are the voltage-dependent rate constants, $k_O(V)$ and $k_C(V)$, for channel opening and closing in which the voltage changes with time we have $k_O(t) = k_O(V(t))$ and $k_C(t) = k_C(V(t))$. In voltage-jump experiments, Eq. (6) leads to single-exponential relaxation with the characteristic time $\tau(V^*)$ that is a function of the voltage V^* at which relaxation is observed, $\tau(V^*) = 1/\left[k_O(V^*) + k_C(V^*)\right]$. It is important that this time is independent of the voltage at which the system was maintained before the jump. In contrast, relaxation toward different applied voltages, for example to closure at −50 mV and to opening at −2.5 mV as shown in Fig. 3a, can differ by orders of magnitude, depending on the sensitivity of the rate coefficients to voltage.

As a particular example, consider the following voltage dependences of the rate coefficients:

$$k_O(t) = k_O^{(0)} \exp\left[\alpha_O V(t)\right],$$
$$k_C(t) = k_C^{(0)} \exp\left[-\alpha_C V(t)\right], \tag{8}$$

where $k_O^{(0)}$ and $k_C^{(0)}$ are the rate constants in the absence of voltage and the positive constants α_O and α_C are inversely proportional to $k_B T$. Such dependences can be interpreted as a consequence of interactions between the charged mobile voltage sensors on the channel-forming protein and the applied electric field (Hille 2001). $k_O^{(0)}$, $k_C^{(0)}$, α_O, and α_C in Eq. (8) are related to the usually reported gating parameters, the gating charge and the voltage of half-effect, by:

$$n = (\alpha_O + \alpha_C)k_B T\big/e,$$
$$V_0 = \frac{1}{(\alpha_O + \alpha_C)} \ln \frac{k_C^{(0)}}{k_O^{(0)}}. \tag{9}$$

This shows that the four parameters are not independent. Obeying the limitations imposed by the experiment (Fig. 2b), $n \simeq 3$ and $V_0 \simeq -30$ mV, as an example, we choose $k_O^{(0)} = 0.305$ s^{-1}, $k_C^{(0)} = 11.6$ s^{-1}, $\alpha_O = 12$ V^{-1}, and $\alpha_C = 108$ V^{-1}. By use of Eqs. (7) and (8) it is easy to see that for this set of values the expected voltage-induced channel opening at $V^* = -2.5$ mV is approximately 20 times faster than closure at $V^* = -50$ mV.

Thus, a crucial experiment to distinguish between the two-state and more complex system is to measure

conductance relaxation at the same voltage for the systems initially kept at different voltages. As discussed above, a "fingerprint" of the two-state system would be the independence of the relaxation times of the initial voltages. To perform such an experiment, we chose an intermediate voltage of -30 mV and studied relaxation of the channel conductance to its stationary value at this voltage from two different initial voltages -2.5 and -50 mV. The results in Fig. 3b illustrate that the characteristic relaxation times of the multi-channel system to its "-30 mV conductance" are approximately hundredfold different, depending on the direction of relaxation. The relaxation time from -2.5 mV is approximately 60 s whereas the relaxation time from -50 mV is approximately 0.8 s. This huge difference in the relaxation times clearly demonstrates the failure of the two-state model.

Finally, we mention that for the two-state system described by Eq. (4) with the rate coefficients given by Eq. (8), analytical results are available for the area encircled by hysteresis curves (Pustovoit et al. 2006). In particular, it was shown that the hysteresis loop area $A(f)$ vanishes as the ramp frequency f tends to zero or infinity, and its asymptotic behavior in the two limiting cases is given by $A(f) \propto f$, as $f \to 0$, and $A(f) \propto 1/f$, as $f \to \infty$. However, no such asymptotic behavior is observed for the experimental data for the loop area presented in Fig. 1c, either at low or high frequencies. We investigated the dependence of area on frequency for different values of the parameters in Eq. (8), which, through Eq. (9), are compatible with the experimentally obtained values of $n \simeq 3$ and $V_0 \simeq -30$ mV, and found that the area can be reasonably well approximated by an empirical dependence $A(f) = A_0/(f/f_0 + f_0/f)$, where A_0 and f_0 are adjustable parameters, with accuracy of 20 % or better (data not shown). This dependence is given as a solid curve in Fig. 1c to demonstrate the discrepancy between the prediction of the two-state model and the experimental data, thus reflecting the complexity of VDAC gating.

Conclusions

We have studied hysteresis in VDAC conductance in response to periodic triangular voltage ramps over a wide range of the ramp frequency, from 0.5 mHz to 0.2 Hz. Rapid relaxation for the opening branches of the hysteresis loops ensures quasi-equilibrium behavior of the channels along these branches and enables simple description of VDAC gating in the framework of a two-state model. In the whole range of ramp frequencies, the gating parameters do not deviate from their average values by more than 15 %. The relaxation-to-the-same-voltage experiment, however, demonstrates conclusively that gating cannot be described

by a two-state Markov model even with the arbitrarily complex dependences of the rate coefficients on voltage. This suggests that VDAC gating is controlled by the dynamics on a multi-dimensional free energy landscape (Frauenfelder et al. 1991). Our tentative conclusion is that when closing and opening, the channels explore different regions of this energy landscape, so that on the way to the closed states the system is far from equilibrium, whereas during opening it mostly follows quasi-equilibrium paths.

References

Andersson T (2010) Exploring voltage-dependent ion channels in silico by hysteretic conductance. Math Biosci 226:16–27

Arbing MA, Hanrahan JW, Coulton JW (2001) Mutagenesis identifies amino acid residues in extracellular loops and within the barrel lumen that determine voltage gating of porin from Haemophilus influenzae type b. Biochemistry 40:14621–14628

Bainbridge G, Gokce I, Lakey JH (1998a) Voltage gating is a fundamental feature of porin and toxin beta-barrel membrane channels. FEBS Lett 431:305–308

Bainbridge G, Mobasheri H, Armstrong GA, Lea EJA, Lakey JH (1998b) Voltage-gating of Escherichia coli porin: a cystine-scanning mutagenesis study of loop 3. J Mol Biol 275:171–176

Banerjee K (2015) Dynamic memory of a single voltage-gated potassium ion channel: a stochastic nonequilibrium thermodynamic analysis. J Chem Phys 142:185101

Bowen KA, Tam K, Colombini M (1985) Evidence for titratable gating charges controlling the voltage dependence of the outer mitochondrial-membrane channel, VDAC. J Membr Biol 86:51–59

Bredin J, Saint N, Mallea M, De E, Molle G, Pages JM, Simonet V (2002) Alteration of pore properties of *Escherichia coli* OmpF induced by mutation of key residues in anti-loop 3 region. Biochem J 363:521–528

Brunen M, Engelhardt H (1993) Asymmetry of orientation and voltage gating of the acidovorax-delafieldii porin Omp34 in lipid bilayers. Eur J Biochem 212:129–135

Colombini M (1989) Voltage gating in the mitochondrial channel, VDAC. J Membr Biol 111:103–111

Colombini M (2004) VDAC: the channel at the interface between mitochondria and the cytosol. Mol Cell Biochem 256:107–115

Colombini M (2012) VDAC structure, selectivity, and dynamics. Biochimica Et Biophysica Acta Biomembranes 1818:1457–1465

Das B, Banerjee K, Gangopadhyay G (2012) Entropy hysteresis and nonequilibrium thermodynamic efficiency of ion conduction in a voltage-gated potassium ion channel. Phys Rev E 86:061915

Delcour AH, Martinac B, Adler J, Kung C (1989) Voltage-sensitive ion channel of *Escherichia Coli*. J Membr Biol 112:267–275

Ehrenstein G, Lecar H, Nossal R (1970) Nature of negative resistance in bimolecular lipid membranes containing excitability-inducing material. J Gen Physiol 55:119–133

Ermishkin LN, Mirzabekov TA (1990) Redistribution of the electric-field within the pore contributes to the voltage-dependence of mitochondrial porin channel. Biochim Biophys Acta 1021:161–168

Flyvbjerg H, Gudowska-Nowak E, Christophersen P, Bennekou P (2012) Modeling hysteresis observed in the human erythrocyte voltage-dependent cation channel. Acta Phys Pol, B 43:2117–2140

Fologea D, Krueger E, Mazur YI, Stith C, Okuyama Y, Henry R, Salamo GJ (2011) Bi-stability, hysteresis, and memory of voltage-gated lysenin channels. Biochimica Et Biophysica Acta Biomembranes 1808:2933–2939

Frauenfelder H, Sligar SG, Wolynes PG (1991) The energy landscapes and motions of proteins. Science 254:1598–1603

Hille B (2001) Ion channels in excitable membranes. Sinauer Associates, Sunderland

Juraszek J, Dybiec B, Gudowska-Nowak E (2005) Hysteresis and synchronization in a two-level system driven by external noise. Fluct Noise Lett 5:L259–L266

Kaestner L, Christophersen P, Bernhardt I, Bennekou P (2000) The non-selective voltage-activated cation channel in the human red blood cell membrane: reconciliation between two conflicting reports and further characterisation. Bioelectrochemistry 52:117–125

Lemasters JJ, Holmuhamedov E (2006) Voltage-dependent anion channel (VDAC) as mitochondrial governator—thinking outside the box. Biochimica Et Biophysica Acta Molecular Basis Disease 1762:181–190

Lemasters JJ, Holmuhamedov EL, Czerny C, Zhong Z, Maldonado EN (2012) Regulation of mitochondrial function by voltage dependent anion channels in ethanol metabolism and the Warburg effect. Biochimica Et Biophysica Acta Biomembranes 1818:1536–1544

Lemeshko VV (2006) Theoretical evaluation of a possible nature of the outer membrane potential of mitochondria. Eur Biophys J Biophys Lett 36:57–66

Lemeshko VV (2014a) VDAC electronics: 2. A new, anaerobic mechanism of generation of the membrane potentials in mitochondria. Biochimica Et Biophysica Acta Biomembranes 1838:1801–1808

Lemeshko VV (2014b) VDAC electronics: 1. VDAC-hexo(gluco) kinase generator of the mitochondrial outer membrane potential. Biochimica Et Biophysica Acta Biomembranes 1838:1362–1371

Mangan PS, Colombini M (1987) Ultrasteep voltage dependence in a membrane channel. Proc Natl Acad Sci U S A 84:4896–4900

Mannikko R, Pandey S, Larsson HP, Elinder F (2005) Hysteresis in the voltage dependence of HCN channels: conversion between two modes affects pacemaker properties. J Gen Physiol 125:305–326

Mathes A, Engelhardt H (1998) Voltage-dependent closing of porin channels: analysis of relaxation kinetics. J Membr Biol 165:11–18

Nestorovich EM, Rostovtseva TK, Bezrukov SM (2003) Residue ionization and ion transport through OmpF channels. Biophys J 85:3718–3729

Peng S, Blachlydyson E, Forte M, Colombini M (1992) Large-scale rearrangement of protein domains is associated with voltage gating of the VDAC channel. Biophys J 62:123–135

Porcelli AM, Ghelli A, Zanna C, Pinton P, Rizzuto R, Rugolo M (2005) pH difference across the outer mitochondrial membrane measured with a green fluorescent protein mutant. Biochem Biophys Res Commun 326:799–804

Pustovoit MA, Berezhkovskii AM, Bezrukov SM (2006) Analytical theory of hysteresis in ion channels: two-state model. J Chem Phys 125:194907

Robertson KM, Tieleman DP (2002) Molecular basis of voltage gating of OmpF porin. Biochem Cell Biol Biochimie Et Biologie Cellulaire 80:517–523

Rostovtseva TK, Bezrukov SM (2012) VDAC inhibition by tubulin and its physiological implications. Biochimica Et Biophysica Acta Biomembranes 1818:1526–1535

Rostovtseva T, Colombini M (1996) ATP flux is controlled by a voltage-gated channel from the mitochondrial outer membrane. J Biol Chem 271:28006–28008

Rostovtseva T, Colombini M (1997) VDAC channels mediate and gate the flow of ATP: implications for the regulation of mitochondrial function. Biophys J 72:1954–1962

Rostovtseva TK, Kazemi N, Weinrich M, Bezrukov SM (2006) Voltage gating of VDAC is regulated by nonlamellar lipids of mitochondrial membranes. J Biol Chem 281:37496–37506

Schein SJ, Colombini M, Finkelstein A (1976) Reconstitution in planar lipid bilayers of a voltage-dependent anion-selective channel obtained from paramecium mitochondria. J Membr Biol 30:99–120

Schindler H, Rosenbusch JP (1978) Matrix protein from *Escherichia Coli* outer membranes forms voltage-controlled channels in lipid bilayers. Proc Natl Acad Sci USA 75:3751–3755

Soares CM, Bjorksten J, Tapia O (1995) L3 loop-mediated mechanisms of pore closing in porin—a molecular-dynamics perturbation approach. Protein Eng 8:5–12

Song JM, Midson C, Blachly-Dyson E, Forte M, Colombini M (1998) The sensor regions of VDAC are translocated from within the membrane to the surface during the gating processes. Biophys J 74:2926–2944

Teijido O, Rappaport SM, Chamberlin A, Noskov SY, Aguilella VM, Rostovtseva TK, Bezrukov SM (2014) Acidification asymmetrically affects voltage-dependent anion channel implicating the involvement of salt bridges. J Biol Chem 289:23670–23682

Thomas L, Blachlydyson E, Colombini M, Forte M (1993) Mapping of residues forming the voltage sensor of the voltage-dependent anion-selective channel. Proc Natl Acad Sci USA 90:5446–5449

VanGelder P, Saint N, Phale P, Eppens EF, Prilipov A, vanBoxtel R, Rosenbusch JP, Tommassen J (1997) Voltage sensing in the PhoE and OmpF outer membrane porins of *Escherichia coli*: role of charged residues. J Mol Biol 269:468–472

Watanabe M, Rosenbusch J, Schirmer T, Karplus M (1997) Computer simulations of the OmpF porin from the outer membrane of *Escherichia coli*. Biophys J 72:2094–2102

Zachariae U et al (2012) Beta-barrel mobility underlies closure of the voltage-dependent anion channel. Structure 20:1540–1549

Zhang DW, Colombini M (1990) Group-Iiia-metal hydroxides indirectly neutralize the voltage sensor of the voltage-dependent mitochondrial channel, VDAC, by interacting with a dynamic binding-site. Biochim Biophys Acta 1025:127–134

Zhou W, Cayabyab FS, Pennefather PS, Schlichter LC, DeCoursey TE (1998) HERG-like K(+) channels in microglia. J Gen Physiol 111:781–794

Zimmerberg J, Parsegian VA (1986) Polymer inaccessible volume changes during opening and closing of a voltage-dependent ionic channel. Nature 323:36–39

Zizi M, Thomas L, Blachlydyson E, Forte M, Colombini M (1995) Oriented channel insertion reveals the motion of a transmembrane beta-strand during voltage gating of VDAC. J Membr Biol 144:121–129

Zizi M, Byrd C, Boxus R, Colombini M (1998) The voltage-gating process of the voltage-dependent anion channel is sensitive to ion flow. Biophys J 75:704–713